



Ultra-Low Loss D-Type Photonic Crystal Fiber Sensor Based on Surface Plasmon Resonance

Shimin Zhu¹ · Xinyu Wang²

Received: 3 April 2024 / Accepted: 27 May 2024

© The Author(s), under exclusive licence to Springer Science+Business Media, LLC, part of Springer Nature 2024

Abstract

A D-type photonic crystal fiber (PCF) sensor with ultra-low loss is presented in this paper. The sensor is capable of detecting analytes in the refractive index (RI) range of 1.36 to 1.42. When the RI of the analyte is 1.36, the maximum loss of the sensor in the x-polarized direction is only 23.25 dB/m. A maximum wavelength sensitivity of 8000 nm/RIU is obtained as the analyte has a RI of 1.42, and the sensor has an average wavelength sensitivity of 4678 nm/RIU in the x-polarization direction. The design of the sensor is implemented by coating the side-polished surface of the PCF with a gold film. For the high-sensitivity sensor, the deposition of gold can provide excellent optical performance while maintaining an ultra-low loss. In general, the designed D-type PCF sensor based on side-polished flat gold layer has great potential in various sensing applications due to its ultra-low loss, high sensitivity, and stable properties.

Keywords Surface plasmon resonance · Photonic crystal fiber · Refractive index sensor · Ultra-low loss

Introduction

Photonic crystal fiber (PCF) is a type of fiber with a variable periodic refractive index (RI) structure that controls and senses light by controlling the optical transmission characteristics of the fiber [1–4]. D-type PCF is also a fiber with a periodic index distribution structure, consisting of a fixed index core and a fiber cladding with a periodic index shift [5]. PCFs with flat, smooth surfaces can be manufactured using side polishing techniques [6]. When incident light passes through the center of the fiber and enters the cladding, due to the change in RI, the light is confined by the periodic structure in the cladding, forming a specific mode, which is often referred to as the SPR mode. This type of sensor is usually fabricated by machining a side-polished structure onto a D-type PCF, which allows light to be transmitted from the inside of the fiber to the external environment, and thus to interact with objects in the environment. When the object

contacts the side-polished part and changes its RI, a change in the transmission properties of the light happens. A signal related to the properties of the object to be measured can be obtained by measuring the changes in the optical transmission properties. Common applications include the measurement of physical parameters such as temperature, pressure, and humidity, and the sensing of chemical substances and biomolecules [7–9]. In summary, a side-polished D-type PCF sensor is a type of sensor based on the fiber structure that uses the variation of the light transmission properties to measure the properties of the object being measured.

In 2022, Saleh Falah et al. proposed a D-shaped PCF surface plasmon resonance (SPR) sensor with open micro-channels [10]. Its RI detection range is between 1.330 and 1.435, with a maximum sensitivity of 28,400 nm/RIU. This sensor has a good linear range and a maximum transmission loss of 22.4 dB/cm. In 2023, Srivastava et al. proposed a sensor probe based on the concept of surface plasmon resonance (SPR) and applied it to the detection of tuberculosis [11]. The sensor probe consists of a D-type PCF and a microscopic elliptical channel. The detection refractive index ranges between 1.343 and 1.351, and the maximum wavelength sensitivity increases to 45,000 nm/RIU. In 2023, Bing et al. proposed a PCF sensor for urine analysis in diabetic patients [12]. Indium tin oxide (ITO) is used as the plasmonic material to be coated on the polishing plane to

✉ Shimin Zhu
zhushimin@neuq.edu.cn

¹ Computing Center, Northeastern University at Qinhuangdao, Qinhuangdao 066004, China

² School of Computer and Communication Engineering, Northeastern University at Qinhuangdao, Qinhuangdao 066004, China

ensure the high flatness of the coating. The maximum wavelength sensitivity is 25,000 nm/RIU in the RI detection range of 1.320–1.355. Overall, side-polished D-type PCF sensors are a promising sensor technology with excellent sensing performance and a wide range of applications, providing an effective solution for high-sensitivity and high-precision fiber sensing [13].

In this paper, we introduce a D-type PCF sensor with ultra-low loss. The sensor is capable of sensing analytes in the RI range from 1.36 to 1.42. In particular, when the RI of the analyte is 1.36, the maximum loss in the x-polarized direction is only 23.25 dB/m. By using simulation calculations, we find that the sensor has an average wavelength sensitivity of 4678 nm/RIU in the x-polarized direction. The sensor is designed by coating the side-polished surface of a PCF with a gold film. The gold film can provide good optical properties while maintaining low-loss properties to achieve high-sensitivity sensors.

Model Design and Operation Principle

Figure 1a shows the end-face structure of a D-type PCF sensor based on a side-polished flat coated gold film. The PCF consists of three layers of air holes of different sizes. The structural parameters of the PCF are as follows: the thickness of the gold film t is 20 nm, the diameter of the large hole d is 2.0 μm , and the diameter of the small hole d_1 is 1.6 μm . The distance h from the polishing surface

of the fiber to the center is 4.0 μm . The distance between two adjacent air holes $\Lambda = 3.0 \mu\text{m}$. The grid structure [14] diagram of the sensor is shown in Fig. 1b.

The gray part in Fig. 1a is the background material of pure silica, whose material dispersion relationship is controlled by the Sellmeier equation:

$$n^2(\lambda) = 1 + \sum_{i=1}^3 \frac{A_i \lambda^2}{\lambda^2 - B_i^2} \tag{1}$$

where $A_1 = 0.6961663$, $A_2 = 0.4079426$, $A_3 = 0.8974794$, $B_1 = 0.0684043 \mu\text{m}$, $B_2 = 0.1162414 \mu\text{m}$, and $B_3 = 9.896161 \mu\text{m}$. The yellow part is the gold film that is applied to the polished surface. Among them, the dielectric constant of gold is calculated using the Drude-Lorentz model:

$$\epsilon_m = \epsilon_\infty - \frac{\omega_D^2}{\omega(\omega + j\gamma_D)} - \frac{\Delta\epsilon \cdot \Omega_L^2}{(\omega^2 - \Omega_L^2) - j\Gamma_L\omega} \tag{2}$$

Here, $\epsilon_\infty = 5.9673$ is the permittivity of gold and $\Delta\epsilon = 1.09$ can be interpreted as the weight factor; ω is the angular frequency of the guiding light. ω_D ($\omega_D/2\pi = 2113.6\text{THz}$) and γ_D ($\gamma_D/2\pi = 15.92 \text{ THz}$) represent the plasma frequency and damping frequency, respectively. Ω_L ($\Omega_L/2\pi = 650.07 \text{ THz}$) and Γ_L ($\Gamma_L/2\pi = 104.86 \text{ THz}$) represent the frequency and spectral width of the Lorentz oscillator, respectively. Here, the loss of optical fiber can be expressed as [15]:

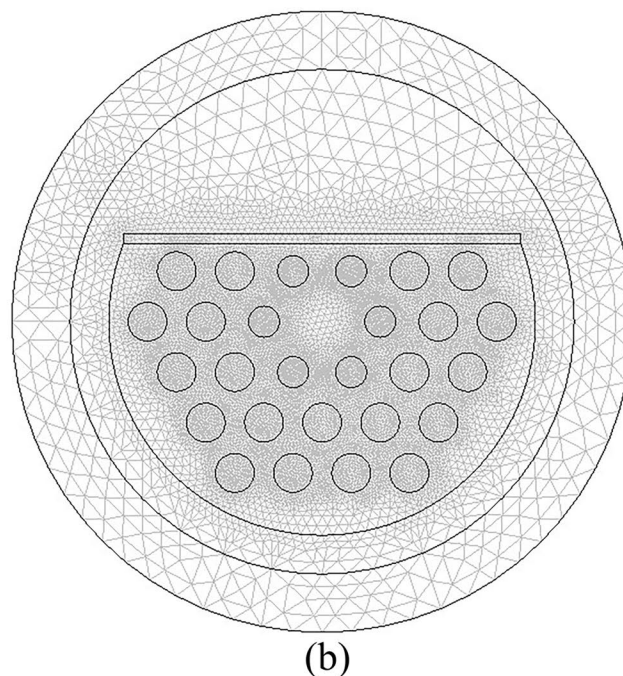
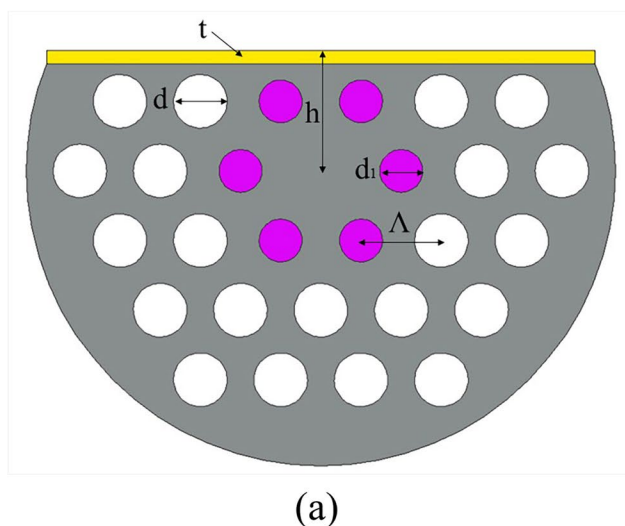


Fig. 1 **a** Cross section of the proposed D-shaped PCF. **b** FEM mesh and scattering boundary condition for computation

$$L = 8.686 \times \frac{2\pi}{\lambda} I_m(n_{\text{eff}}) \times 10^6 \tag{3}$$

where λ represents the wavelength of light and $I_m(n_{\text{eff}})$ represents the imaginary part of effective refractive index. The loss unit is dB/m and the wavelength unit is μm .

When the RI of the analyte is 1.38, the relationship between the confining losses of x-polarized (black curve) and y-polarized light (red curve) in the fiber core and the wavelength is shown in Fig. 2, which clearly shows that the confining loss in the y-polarized direction is much higher than that in the x-polarized direction. In particular, the confining loss in the y-polarized direction increases with wavelength. In the inset of Fig. 2, it is clear to understand the dependence of the limiting loss of x-polarized in the fiber core on the change in wavelength. The data show that the limiting loss of the x-polarized fiber core mode reaches its

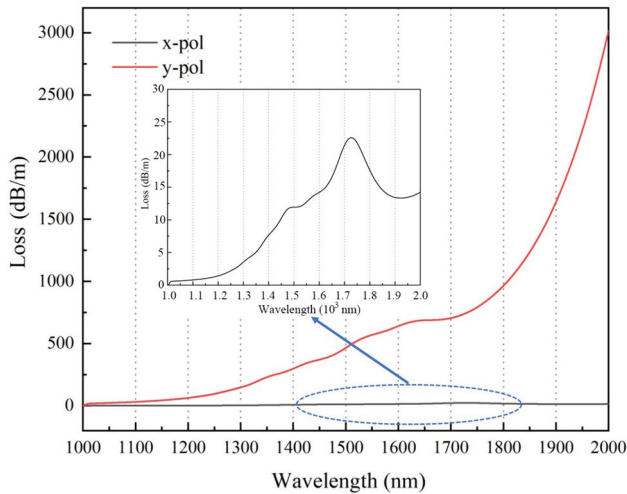
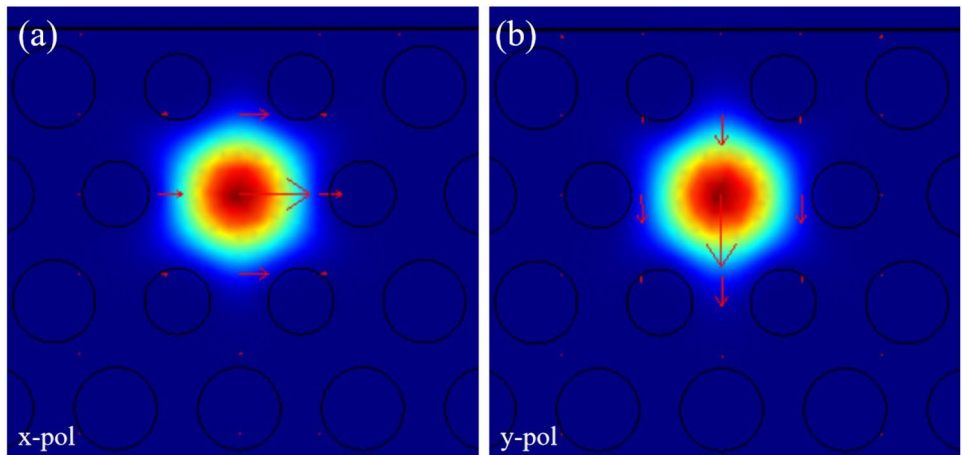


Fig. 2 The loss of the core mode with a refractive index of 1.38 as a function of wavelength

Fig. 3 a, b Electric field distribution of x-polarized and y-polarized core mode at wavelengths of 1730 nm, respectively



maximum value of 22.62 dB/m at the resonance wavelength of 1730 nm. Therefore, in the following analysis of the sensing performance of the sensor, the x-polarization direction will be the object of study.

Figure 3a and b show the electric field distribution in x-polarization direction and y-polarization direction at the wavelength of 1730 nm, respectively [16]. As shown in Fig. 3, from the mode field distribution of the x- and y-polarized fiber core modes, it is clear that most of the energy is bound in the fiber core and therefore the corresponding confining losses are very low.

Here, by choosing a suitable thickness of the metallic film, the sensor can be made more sensitive to a particular target material. Adjusting the size of the air holes around the fiber can affect the performance of the sensor, just as changing its optical properties by tailoring the core and cladding refractive indices of the fiber. Thus, by tuning structural parameters such as the thickness of the metal film and the size of the air holes, the performance of D-type plasmonic resonant fiber sensors can be optimized and their selectivity towards the target material can be improved.

Simulation Results and Discussion

Figure 4a–d shows the numerical simulation results of the loss of the x-polarized core mode as a function of wavelength when the thickness t of the plasmonic material gold film is 20, 30, 40, and 50 nm, respectively. The data show that for the same thickness of the gold film, the resonance wavelength in the x-polarization direction shifts towards the longer wavelength direction as the refractive index increases, the loss intensity gradually decreases, and the width of the half-peak of the loss peak widens. When the thickness of the gold film is $t = 20$ nm, the sensor has the widest range of refractive index detection, ranging from 1.36 to 1.42. When the thickness of the gold film is $t = 30$ nm, the refractive

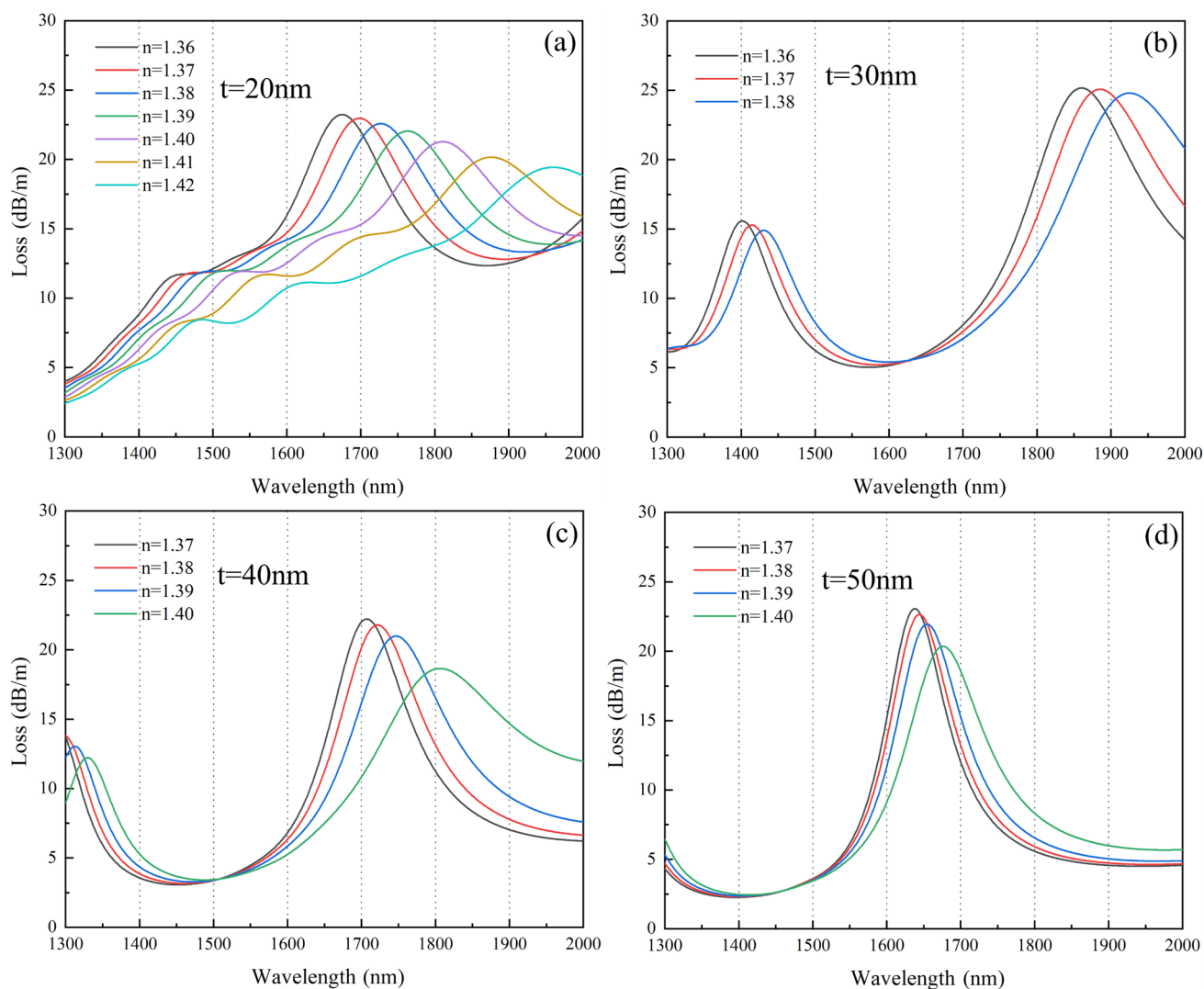


Fig. 4 a–d The relationship between the loss of the x-polarized core mode and wavelength variation, with thicknesses t of 20, 30, 40, and 50 nm, respectively

index detection range of the sensor is 1.36 to 1.38. When the thickness of the gold film is $t = 40$ nm, the refractive index detection range of the sensor is 1.37 to 1.40. When the thickness of the gold film is $t = 50$ nm, the refractive index detection range of the sensor is 1.37 to 1.40. Therefore, a gold film thickness of $t = 20$ nm is the optimal structural parameter for this sensor.

The air hole diameter of 1.6, 1.8, and 2.0 μm was selected and its effect on loss was investigated. The loss of the x-polarization core mode of the D-type PCF sensors with the wavelength is shown in Fig. 5a–c, respectively. It can be seen that the resonant wavelength in the x-polarized direction is shifted towards the long wavelength direction as the RI increases for the same diameter. At the same time, the intensity of the loss gradually decreases and the half-peak width of the loss peak becomes wider. At different

diameters, it is observed that the resonance wavelength of the x-polarized fiber core mode is blue-shifted with increasing pore diameter, the loss intensity gradually decreases, and the overall half-peak width of the loss peak broadens. In addition, we investigate the effect of different aperture diameters on the range of RI detection of the sensor. When the diameter of the pore is 1.6 μm , the RI of the analyte ranges from 1.36 to 1.42. When the diameter of the hole is 1.8 μm , the RI detection range of the sensor is 1.36–1.42. When the aperture diameter is 2.0 μm , the sensor RI detection range is 1.36–1.41. In summary, the diameter of 1.6 μm is the best structural parameter of the sensor.

Figure 6 shows that the normalized transmission power decreases as the length of the PCF sensing region increases, while the position of the resonant absorption peak remains almost constant, similar results were also observed in

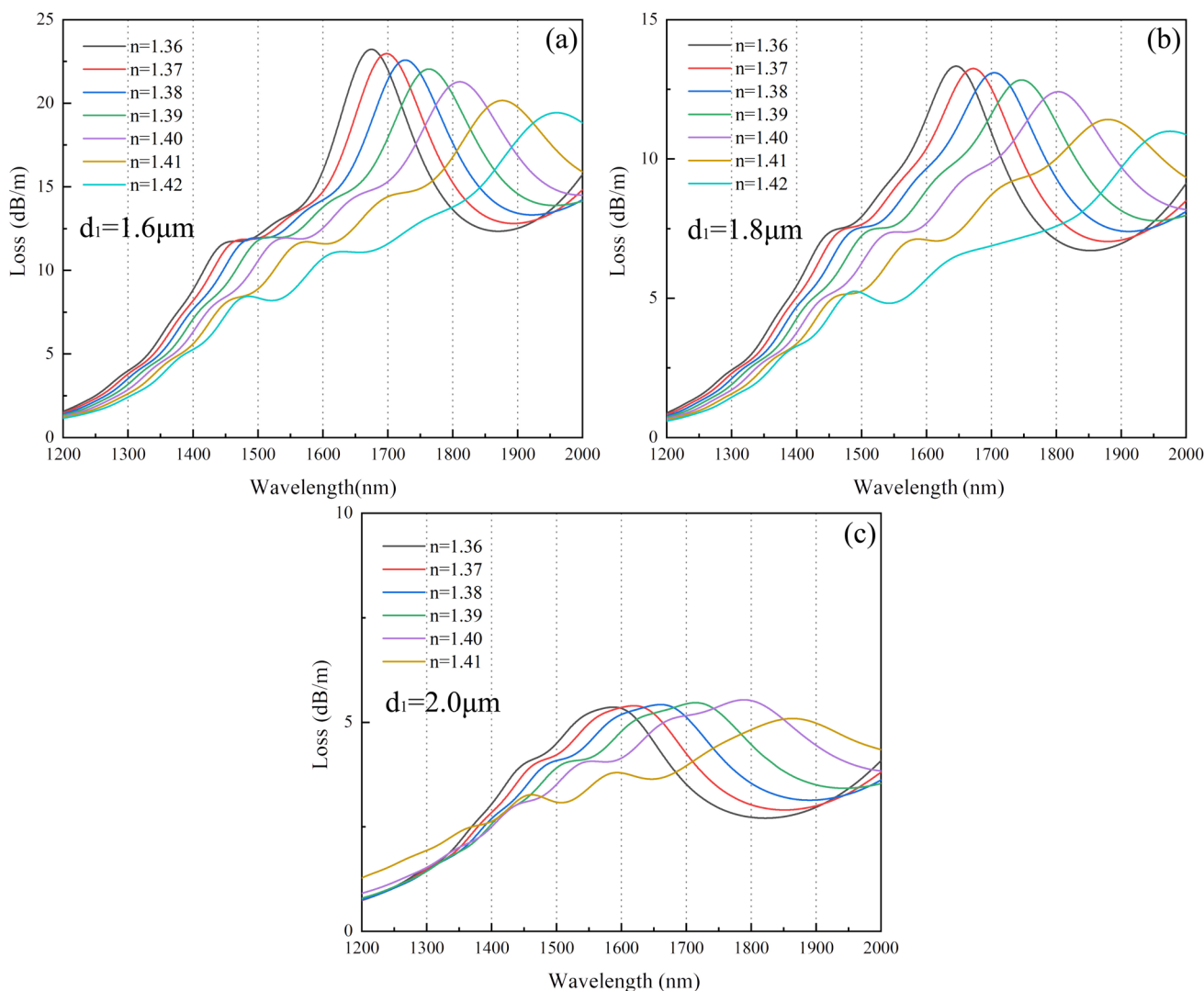


Fig. 5 a–c The relationship between the loss of the x-polarized core mode and wavelength variation, with diameter d_1 of 1.6, 1.8, and 2.0 μm , respectively

reported works [17]. This indicates that the length of the PCF polishing region can be increased appropriately, while maintaining the wavelength sensitivity of the sensor, which is beneficial for practical applications of the sensor. When the length of the sensing region is shortened from 300 to 50 mm, the loss absorption peak at the resonance wavelength remains is sharp, indicating that shortening the length of the polishing region does not affect the discrimination of the sensing detection.

Therefore, the optimal structure of the designed PCF sensor is obtained through calculation; that is, the thickness of the gold film is 20 nm, the diameter of the small hole is 1.6 μm , and the sensor can detect the RI of the analyte from 1.36 to 1.42. Wavelength sensitivity is an important index used to evaluate sensor performance, which can be calculated by the following formula [18]:

$$S_\lambda(nm \cdot RIU^{-1}) = d\lambda_{peak}/dn_a \tag{4}$$

where $d\lambda_{peak}$ represents the wavelength change under the change of unit RI, and dn_a represents the change of unit RI.

Figure 7a and b show the linear fitting results of the x-polarization core mode loss characteristic curve and wavelength sensitivity of the D-type sensor with the thickness of the gold film of 20 nm and the diameter of the holes near the core of 1.6 μm , respectively. According to the fitting results [19], the average wavelength sensitivity of the D-type sensor is 4678.57 nm/RIU. A linear fit gives a value of 0.94305. The parameters and simulation results are shown in Table 1. The performance comparison of the designed D-type photonic crystal fiber sensor with some reported PCF-based SPR sensors are presented in Table 2 [20–23]. It can be observed that the sensing performance of our proposed PCF-based SPR

Fig. 6 Normalized transmission spectra for several polish lengths of the D-type sensor

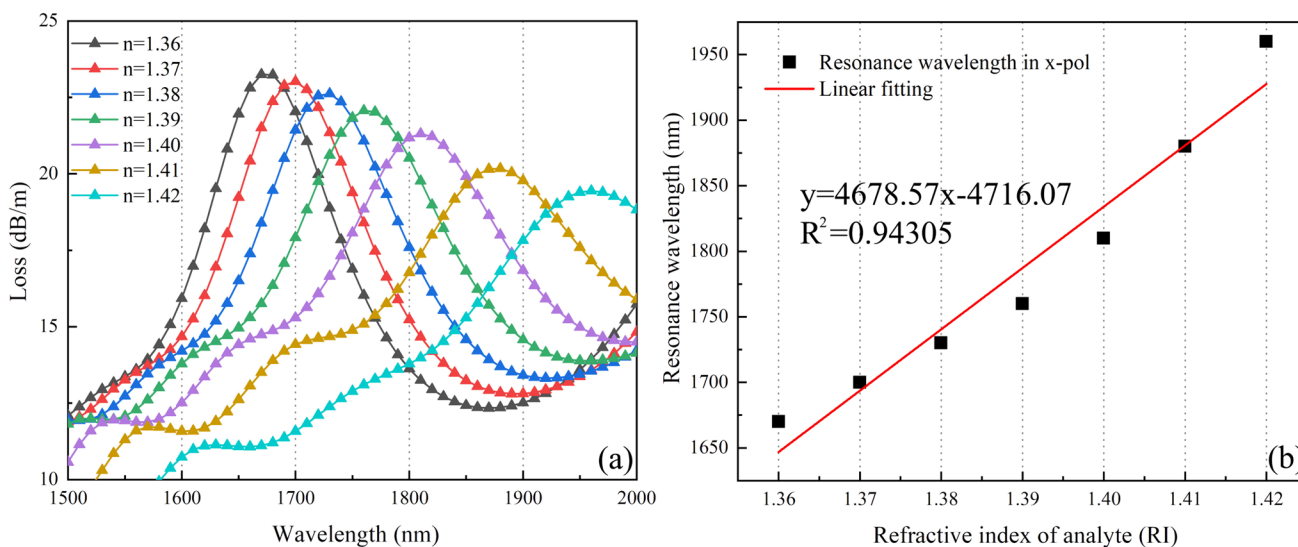
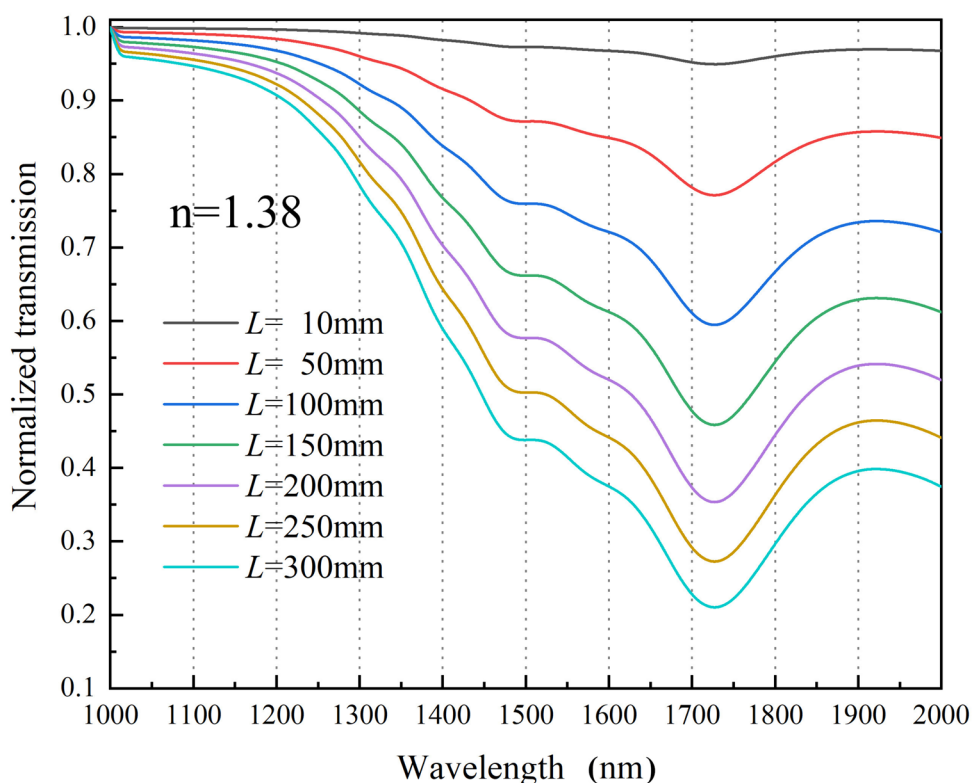


Fig. 7 **a** Loss curves corresponding to different refractive indices. **b** Linear fitting results of refractive index and resonance wavelength

Table 1 Simulation results of the proposed D-type sensor

Gold film thickness (t)	20 nm
Small hole diameter (d_1)	1.6 μm
Fiber loss	≤ 23.25 dB/m
Refractive index range	1.36–1.42
Average wavelength sensitivity	4678.57 nm/RIU
Maximum wavelength sensitivity	8000.00 nm/RIU

sensor is significantly optimized and improved as compared with reported results [20–23].

Table 2 Sensitivity comparison of this work with recently reported fiber optic sensors

Fiber type	Wavelength range (nm)	RI range (RIU)	Sensitivity (nm/RIU)	Ref.
PCF with a 12-fold symmetry	450–650	1.31–1.34	1172	[20]
PCF coated with silver film	500–900	1.333–1.3953	3341.65	[21]
Localized SPR fiber sensor	800–1000	1.374–1.391	3953	[22]
MoO ₂ -deposited C-shaped PCF sensor	900–1300	1.31–1.37	4821	[23]
Low loss D-shaped PCF	1500–2000	1.36–1.42	4678.57	This work

Conclusion

A D-type PCF sensor with ultra-low loss has been proposed. This sensor is capable of sensing and detecting analytes with refractive indices ranging from 1.36 to 1.42. This sensor has a maximum loss of only 23.25 dB/m in the x-polarization direction. The average wavelength sensitivity reaches 4678 nm/RIU. The design of the sensor is achieved by coating a gold film on the side-polished surface of the PCF. Such coatings can provide good optical performance while maintaining low-loss properties, enabling high-sensitivity sensors with great potential for various sensing applications.

Author Contribution All authors contributed to the study conception and design. S.M. Zhu: conceptualization, methodology, software, writing — original draft. X.Y. Wang: resources, and software, writing — reviewing. All authors read and approved the final manuscript.

Funding This work is supported by the Postdoctoral Preferred Funding Research Project of Hebei Province (Grant No. B2018003008) and the Fundamental Research Funds for the Central Universities of China (Grant No. N2123008).

Data Availability No datasets were generated or analysed during the current study.

Declarations

Competing Interests The authors declare no competing interests.

References

1. Qian Z, Yang W, Wu D, Ding L (2023) Low-loss flexible terahertz photonic crystal fiber. *Opt Eng* 62:026103. <https://doi.org/10.1117/1.OE.62.2.026103>
2. Wang E, Han Q, Zhou X, Yuan H, Li J (2022) A Bend-resistant Photonic Crystal Fiber with large effective Mode Area. *Opt Fiber Tech* 71:102902. <https://doi.org/10.1016/j.yofte.2022.102902>
3. Fu X, Zhang Y, Zhang W, Zhang Y, Jin W, Fu G et al (2022) A coaxial torsion sensor based on intermodal interference in Grapefruit microstructured fiber. *Opt Commun* 521:128573. <https://doi.org/10.1016/j.optcom.2022.128573>
4. Liu X, Yuan J, Qu Y, Zhang J, Zhou X, Yan B et al (2023) D-shaped photonic crystal fiber sensor based on the surface plasmon resonance effect for refractive index detection. *Appl Opt* 62:E83. <https://doi.org/10.1109/jphot.2018.2790424>
5. Yang D, Huang J, Xu B, Lv G, Li Y, Cheng T (2023) Design of high-performance photonic crystal fiber polarization filter by Grey Wolf Optimizer with convolutional neural network. *Optik* 283:170925. <https://doi.org/10.1016/j.ijleo.2023.170925>
6. Zhuo L, Tang J, Zhu W, Zheng H, Guan H, Lu H et al (2023) Side polished Fiber: a versatile platform for Compact Fiber devices and sensors. *Photonic Sens* 13:230120. <https://doi.org/10.1007/s13320-022-0661-x>
7. Yan L, Wang Q, Yin B, Xiao S, Li H, Wang M et al (2023) Research on simultaneous measurement of magnetic field and temperature based on petaloid photonic crystal fiber sensor. *Sensors* 23:7940. <https://doi.org/10.3390/s23187940>
8. Bock W, Chen J, Eftimov T, Urbanczyk W (2006) A photonic crystal Fiber sensor for pressure measurements. *IEEE T Instrum Meas* 55:1119. <https://doi.org/10.1109/TIM.2006.876591>
9. Gao P, Zhou Y, Fu T, Cao Y, Zheng X, Liu Y et al (2024) U-shaped PCF humidity sensor coated with polyvinyl alcohol. *Mod Phys Lett B*. <https://doi.org/10.1142/S0217984924500891>
10. Falah AAS, Wong W, Mahdiraji GA, Adikan FRM (2022) Single-mode D-shaped photonic crystal fiber surface plasmon resonance sensor with open microchannel. *Opt Fiber Technol* 74:103105. <https://doi.org/10.1016/j.yofte.2022.103105>
11. Srivastava R, Pal S, Prajapati YK (2023) MXene-assisted D-shaped photonic crystal fiber probe with high sensitivity for detection of tuberculosis. *Plasmonics* 18:2049. <https://doi.org/10.1007/s11468-023-01924-8>
12. Bing P, Zhao J, Liu Q, Yi X, Li Z, Zhang H et al (2023) Photonic crystal fiber-based plasmonic sensor with ITO for medical applications. *Eur Phys J D* 77:68. <https://doi.org/10.1140/epjd/s10053-023-00655-z>
13. Islam N, Arif MFH, Yousuf MA, Asaduzzaman S (2023) Highly sensitive open channel based PCF-SPR sensor for analyte refractive index sensing. *Results Phys* 46:106266. <https://doi.org/10.1016/j.rinp.2023.106266>
14. Zhang S, Li J, Li S, Liu Q, Liu Y, Zhang Z, Wang Y (2018) A tunable single-polarization photonic crystal fiber filter based on surface plasmon resonance. *Appl Phys B-Lasers Opt* 124:112. <https://doi.org/10.1007/s00340-018-6988-8>
15. Zhang S, Li J, Li S (2018) Design and numerical analysis of a novel dual-polarized refractive index sensor based on D-shaped photonic crystal fiber. *Metrologia* 55:828. <https://doi.org/10.1088/1681-7575/aae757>
16. Salimullah SM, Faisal M (2023) Ultra-wideband and coherent super continuum generation (near and mid-infrared) in dispersion flattened ZnGeP₂ photonic crystal fiber. *Alex Eng J* 70:289. <https://doi.org/10.1016/j.aej.2023.03.002>
17. Zhang S, Li J, Liu Q, Wu J, Guo Y (2018) Surface plasmon resonance sensor based on D-shaped photonic crystal fiber with two micro-openings. *J Phys D: Appl Phys* 51:305104. <https://doi.org/10.1088/1361-6463/aae72>

18. Ehyae A, Mohammadi M, Seifouri M, Olyae S (2023) Design and numerical investigation of a dual-core photonic crystal fiber refractive index sensor for cancer cells detection. *Eur Phys J Plus* 138:129. <https://doi.org/10.1140/epjp/s13360-023-03749-0>
19. Sorathiya V, Lavadiya S, Faragallah OS, Eid MMA, Rashed ANZ (2022) D shaped dual core photonics crystal based refractive index sensor using graphene–titanium–silver materials for infrared frequency spectrum. *Opt Quant Electron* 54:290. <https://doi.org/10.1007/s11082-022-03700-0>
20. Mahsa A, Mohammad H (2022) Photonic quasi–crystal fiber–based plasmonic biosensor: a platform for detection of coronavirus. *Plasmonics* 17:1655. <https://doi.org/10.1007/s11468-022-01651-6>
21. Gao Z, Feng Y, Chen H, Chen Q, Li Y, Zhang M (2023) Refractive index and temperature sensing system with high sensitivity and large measurement range using an optical fiber. *IEEE Trans Instrum Measurement* 72:9502706. <https://doi.org/10.1109/TIM.2023.3237224>
22. Jia S, Ma A, Dong H, Xia S (2022) Quantifiable effect of inter-particle plasmonic coupling on sensitivity and tuning range for wavelength-mode LSPR fiber sensor fabricated by simple immobilization method. *Sensors* 22:9075. <https://doi.org/10.3390/s22239075>
23. Dong J, Zhang S (2023) Characteristics of MoO₂ deposited C-shaped photonic crystal fiber sensor with a micro-opening based on surface plasmon resonance. *Plasmonics* 18:1971. <https://doi.org/10.1007/s11468-023-01918-6>

Publisher's Note Springer Nature remains neutral with regard to jurisdictional claims in published maps and institutional affiliations.

Springer Nature or its licensor (e.g. a society or other partner) holds exclusive rights to this article under a publishing agreement with the author(s) or other rightsholder(s); author self-archiving of the accepted manuscript version of this article is solely governed by the terms of such publishing agreement and applicable law.